Liquid Crystals
Publication details, including instructions for authors and subscription information:
http://www.informaworld.com/smpp/title~content=t713926090

Liquid crystal orientation by holographic phase gratings recorded on photosensitive Langmuir-Blodgett films

L. M. Blinov

Online publication date: 06 August 2010

To cite this Article Blinov, L. M.(1999) 'Liquid crystal orientation by holographic phase gratings recorded on photosensitive Langmuir-Blodgett films', Liquid Crystals, 26: 3, 427 — 436
To link to this Article: DOI: 10.1080/026782999205209
URL: http://dx.doi.org/10.1080/026782999205209

LIQUID CRYSTALS, 1999, VOL. 26, NO. 3, 427–436

Liquid crystal orientation by holographic phase gratings recorded on photosensitive Langmuir–Blodgett films

L. M. BLINOV†*‡, R. BARBERI†, G. CIPPARRONE†, M. IOVANE†,
A. CHECCO†, V. V. LAZAREV† and S. P. PALTO‡

†Istituto Nazionale di Fisica della Materia, c/o Dipartimento di Fisica,
Universitá della Calabria, I-87036, Rende (Cs), Italy
‡Institute of Crystallography, Russian Academy of Sciences, 117333 Moscow,
Leninsky prosp. 59, Russia

(*Received 24 July 1998; accepted 17 September 1998*)

Holographic gratings were recorded on photosensitive Langmuir–Blodgett films characterized by UV spectroscopy, birefringence measurements and atomic force microscopy. Different polarizations of Ar laser writing beams create particular patterns of chromophore orientation in the diffraction spots. The gratings were shown to orient a nematic liquid crystal with the director parallel to the axes of the chromophores predetermined by film irradiation. In the case of the *sp* grating (recorded with laser beams polarized perpendicular to each other), two equivalent easy directions for the liquid crystal orientations at 90° with respect to each other were observed; that is a quasi-bistable anchoring interface had been prepared. Measurements of the pretilt angles ϑ_s and anchoring energy W_s of 5CB on different holographic gratings show that this orientation technique is very promising for display technology.

1. Introduction

Electro-optical effects in nematic liquid crystals are widely used in display technology [1]. The character of an effect used is mostly determined by the dielectric anisotropy of a liquid crystal and the boundary conditions at the solid substrates that form a plane cell capillary filled with the substance. For orientation of liquid crystals, special thin orienting layers must be prepared and, to this end, several methods have been suggested. For cells with planar homogeneous orientation at opposite substrates (e.g. for twist cells) the most popular techniques are the oblique evaporation of SiO and the buffing of thin spin-coated polymer (e.g. polyimide) layers. More recently, for the same purpose, polarized light treatment of photopolymers [2, 3] or dye doped polymers [4] has been suggested. For cells with homeotropic orientation, as a rule, a deposition of surfactant layers is used.

Liquid crystals may also be oriented by a wave-like relief on the solid surface. Such a relief may be prepared by a photolithographic grating technique using optically isotropic photoresists in the form of spin-coated films [5]. In this case, in order to reduce the elastic energy, a liquid crystal is oriented along the grooves, that is perpendicular to the wave vector $\mathbf{q}$ of the grating. The predicted efficiency of the liquid crystal orientation [6] depends on the wavevector (proportional to $\mathbf{q}^3$) and the amplitude (proportional to A^2) of a relief, and, in some cases, this agrees with experimental data [7]. A liquid crystal orienting relief may also be created by scans using an atomic force microscope (AFM) [8]. Recently bistable gratings were suggested [9] where two gratings with perpendicular wave vectors overlapped each other and created two easy directions for liquid crystal orientation. Such substrates are of great interest for the development of novel displays based on bistability phenomena [10].

A paper by Gibbons *et al.* [4] was for a long time the only account of liquid crystal orientation being observed on a holographic grating. The grating was created by visible light absorbed in a layer of a polymer doped with a photochromic azo-dye. Data related to the strength of liquid crystal anchoring on gratings and other details (like pretilt angles) have not yet been reported. Such data may only be found for a UV sensitive polymer (polyvinyl cinnamate) irradiated by a uniform light beam (without grating formation) [11, 12].

In our opinion, the potential of Langmuir–Blodgett (LB) films as orienting layers for liquid crystals is not yet well understood. The very first studies on this subject were carried out in the seventies [13]. Depending on the molecular structure of the films, they may provide either

*Author for correspondence.

Journal of Liquid Crystals ISSN 0267-8292 print/ISSN 1366-5855 online
http://www.tandf.co.uk/JNLS/lct.htm
http://www.taylorandfrancis.com/JNLS/lct.htm

homeotropic or planar homogeneous orientation [14–18]. The work of Ishimura *et al.* [19, 20] stimulated great activity on investigations of liquid crystal orientation on so-called 'command surfaces' where the microstructure of an orienting film was controlled by light. In some studies [19, 20] unpolarized light of different wavelengths was used to cause a reversible *trans–cis–trans*-isomerization in azobenzene chromophores chemically attached to amphiphilic molecules forming Langmuir–Blodgett films. Such surfaces are isotropic in the plane of a substrate. On the other hand, it has been shown [21] that LB films composed of amphiphilic azo-dye molecules manifest a phenomenon of photoinduced molecular reorientation: on irradiation with linearly polarized light within the azo-chromophore absorption band, initially optically isotropic films (in their plane) become dichroic and birefringent due to the azo-chromophore reorientation predominantly perpendicular to the light polarization vector.

Up to now, however, there are only a few papers devoted to orientation of liquid crystals by this system. It has been shown that irradiated films orient nematic liquid crystals unidirectionally along the azo-chromophore axes. Moreover, in some special cases (double irradiation with different light polarizations) the films may provide two easy directions for liquid crystal orientation (bistable surface [22]). The performance characteristics of electro-optical cells with liquid crystals oriented by photosensitive LB films seem to be very promising [23]. Holographic diffraction gratings were shown to be easily recorded in such films [24], and a preliminary attempt to observe liquid crystal orientation on such a grating was also reported [23].

The aim of the present paper is to study liquid crystal orientation on photosensitive LB films in more detail. First we characterize the LB film gratings by several techniques (absorption spectroscopy, birefringence, AFM, diffraction efficiency), then we study the orientation of a liquid crystal on the gratings recorded with different light polarizations (*ss*, *pp*, *sp*) and describe a special case of a quasi-bistable orientation, and finally we measure the anchoring energy and pretilt angles for different gratings.

2. Experimental techniques

2.1. *LB films and grating preparation*

The films were prepared from an amphiphilic dye MEL63 (NIOPIK, Moscow). The molecule contains an azobenzene chromophore, a polar head (–COOH) with electron acceptor properties and a hydrophobic tail ($-NHC_9H_{19}$) with electron donor properties, figure 1. The azobenzene chromophore in its extended, *trans*-isomeric state acts as an electronic oscillator along its molecular longitudinal axis and absorbs light in the spectral region 400–500 nm.

The LB films were prepared using successive transfer of molecular layers from the water surface onto a glass substrate. We used indium tin oxide (ITO) coated glass plates that turned out to be hydrophobic. The dye molecules spontaneously form crystallized ('solid') films on a water surface, and for this reason we used the Langmuir–Schäfer method to prepare multilayer films. To prevent air bubbles, the substrate was put in contact with the water with its plane making a small angle with respect to the surface. It is still a delicate process to prepare highly homogeneous films. We have found that it is better not to use the traditional compression of a

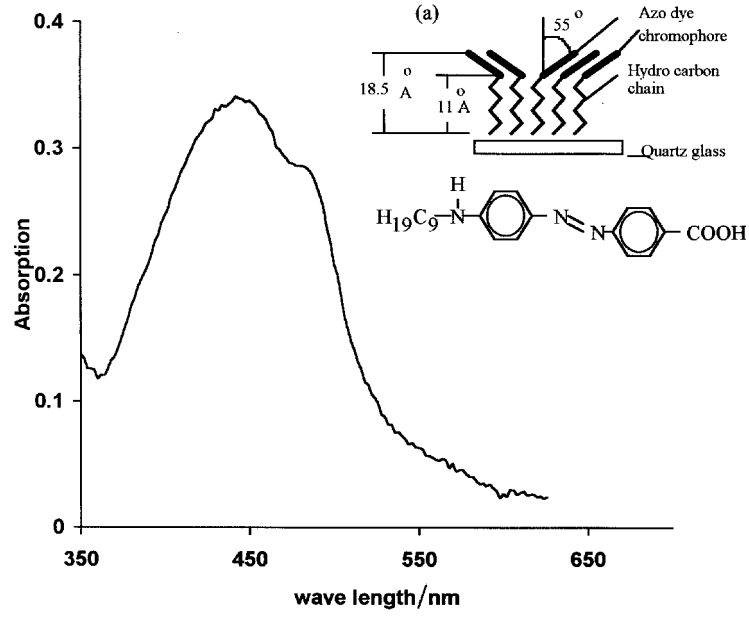

Figure 1. Absorption spectrum of an 8 bilayer thick film of MEL63 and a structure on an X-type monolayer of the MEL-63 azo-dye molecules shown alongside.

film by a barrier, but to operate with a limited spreading area of water (about 400 cm^2). The following procedure seems to provide optimum homogeneous films: a 0.01 wt % solution of the dye in chloroform is poured continuously onto the water surface at a rate of 0.1 ml min^{-1}. A dye layer shows high reflectivity in the visible region of the spectrum, and therefore during solution spreading one can easily observe the process of crystallization. The crystallized film, having most probably a bilayered structure, occupies a larger free area when more material is added, and we stopped the spreading procedure when the film covered almost all the available surface.

Five transferred bilayers are sufficient to orient NLC molecules. Nevertheless, to have better orientation we used films consisted of 10–15 bilayers. X-ray investigations and out-of-plane dichroism data show that, in a transferred film, the azo-chromophore axes deviate from the film normal by an angle ϑ of about 60° [22]. This is schematically shown in figure 1 (*a*). On film irradiation, the chromophores are predominantly reoriented around the film normal along a conical surface as in a smectic C liquid crystal.

A serious problem is the measurement of film thickness. A standard profilometer cannot be used due to the softness of the transferred films. Therefore, the thickness was measured by non-destructive methods, either using an interference microscope MII-4, Russia (films thicker than 2000 Å) or by atomic force microscopy with an Autoprobe CP, Park Scientific Instruments (thin films, 10–500 Å).

The surfaces of soft samples can be investigated on a sub-micron scale using the 'non-contact' AFM mode, when the probing tip moves along the surface at such a distance that no physical contact occurs and long range van der Waals forces between tip and sample are measured. A sample is mounted on an X, Y, Z piezo stage with the tip-surface distance Z varied during the 10 μm × 10 μm X-Y scan in order to keep constant the force acting on the tip (this means a constant feedback current). The voltage applied to the Z-piezo driver is the signal to be measured, which gives, after proper calibration, the profile of the surface.

For all the films the absorption spectra were measured with a standard spectrometer Cary 5E (Varian). Virgin films showed no birefringence. The polarized light absorbed by azo-chromophores induces an optical anisotropy, and, with the thickness known, the optical anisotropy may be found from the phase delay measured by polarizing microscopy aided by a compensator. For our measurements a variable tilt compensator (Zeiss E) introduced into the polarizing microscope (Axioskop, Zeiss) was used.

For recording and characterization of holographic gratings we used a simple pump and probe technique, shown in figure 2. In order to write a grating, a configuration of the Michelson interferometer was used: a beam of an Ar-ion laser (model Coherent T90) of wavelength $\lambda_w = 515$ nm was split into two beams and sent to a sample at a small angle $\Theta \approx 2.8°$. The light power could be changed from 1 mW to 100 mW. The polarizations of the two converging beams were installed separately with the help of $\lambda/2$ plates and Glan–Thomson prisms and we could record *ss*, *pp* and *sp* gratings. The *s*- and *p*-polarizations correspond to the light electric vector **e** perpendicular and parallel, respectively, to the plane of light incidence on the sample. The latter is horizontal in our experimental set-up. The illuminated spot at the sample was about 1.6 mm in diameter. The grating period is determined by the angle Θ and equals 10 μm (for details, see [24]). As a reference, some spots were recorded with one beam (*s* or *p* spots, no grating).

To characterize a grating, a probe (reading) beam of a He-Ne laser ($\lambda_r = 6328$ Å) with controlled polarization was sent into the same spot normally to the film surface and detected by a Si photodiode behind the sample and a pinhole. The diffraction efficiency η_n of the grating was calculated as the ratio I_n/I_0 where I_0 and I_n are the intensities of the incident light and the light in the nth diffraction order. The induced birefringence was measured by microscopy, as explained above, separately for each set of the alternating stripes. The images of gratings were recorded by a Panasonic Colour CCTV Camera (Model WV-CL700/G) connected to a PC.

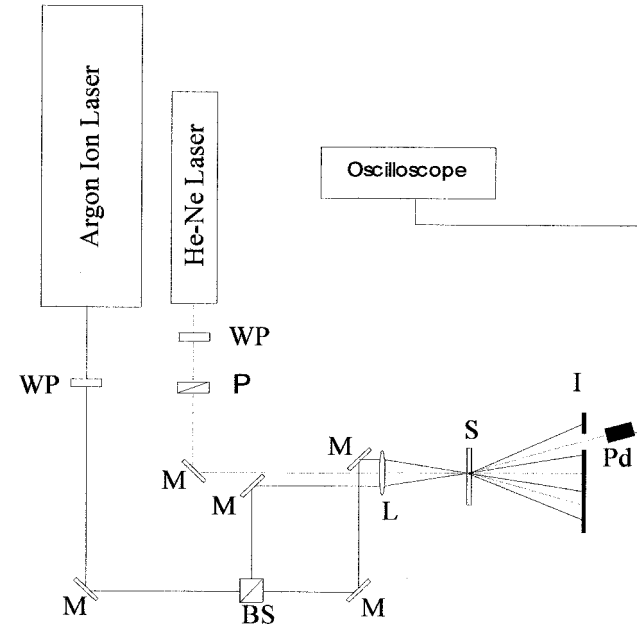

Figure 2. The pump and probe technique for writing, reading-off and erasing a diffraction grating. WP: $\lambda/2$ wave plates; M: mirrors; BS: beam splitter; P: polarizer; L: lens; S: sample; I: iris; Pd: photodiode.

2.2. *Liquid crystal cells*

The serious problem was solubility of our LB films in the liquid crystal. To avoid this, after polarized light treatment, we irradiated films additionally for 30 min with UV light from a mercury lamp with total light power density of about 20 mW cm^{-2}. Such a treatment considerably reduced solubility of the film in organic solvents, probably due to formation of molecular dimers or larger aggregates by hydrogen bond formation between carboxyl groups. Finally the film was etched in a hexane–toluene mixture with a few drops of acetone in order to remove the remaining soluble parts of the film.

Hybrid liquid crystal cells of 10–30 μm thickness were made as usual with two teflon strips separating the two substrates. One of the substrates had a light processed LB film as a planarly orienting layer; the ITO electrode of the opposite substrate was covered with a surfactant, dimethyloctadecyl-3-(trimethoxysilyl)propylamonium chloride, DMOAP, to provide a homeotropic orientation with strong anchoring of the director. The cells were filled with 4-pentyl-4′-cyanobiphenyl, 5CB, in the isotropic phase, in order to minimize orientation of the liquid crystal by flow. For the sake of comparison, several irradiated spots (*s*, *p*, *ss*, *pp*, *sp*) were prepared in the same cell. The cell textures were studied under the same polarizing microscope equipped with a compensator. The technique allowed us to determine the direction of the easy axes, the local values of the birefringence across a grating and the pretilt angle at the grating interface. The anchoring energy was measured by a newly developed technique [25] based on a modification of Yang's theoretical approach [26] for a semi-infinite planar layer.

3. Results and discussion

3.1. *Properties of LB films*

An optical spectrum of a virgin LB film consisting of 8 bilayers is shown in figure 1. Two absorption bands typical of the aggregated state of amphiphilic azo-compounds [24, 27] are clearly seen. The long wave band centred at 460 nm is more sensitive to Ar-laser light than the short wave band centred around 440 nm [24]. The film consists of a number of small domains of a few micrometres in size as can be seen in the picture taken by AFM, figure 3 (*a*). The thickness of the film was measured by the same AF microscope. First, a thin scratch was produced by the stylus of a profilometer, and then a scan by AFM was made across the scratch.

The dependence of the film thickness on tip position is shown in figure 3 (*b*) for a film consisting of 8 bilayers. The depth of the scratch taken from the figure is 380 ± 50 Å, and so the thickness of one bilayer is found,

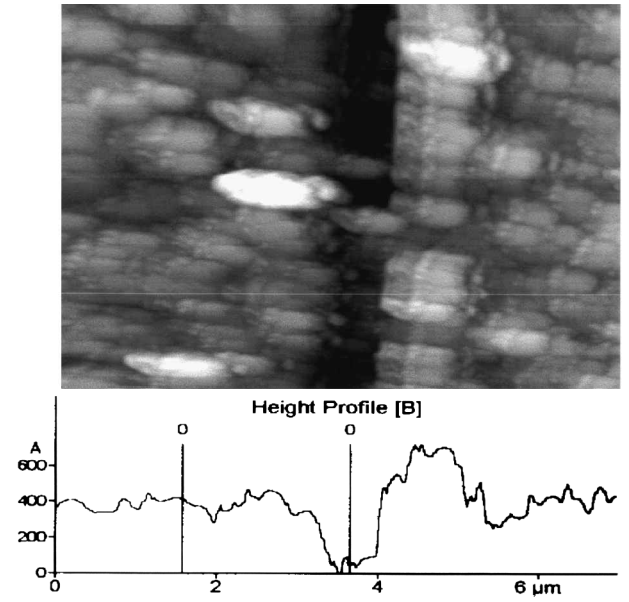

Figure 3. Domain structure of a MEL63 film observed with the non-contact AFM mode (top) and the height profile of the film across the scratch, along line B (bottom).

$d_b \approx 47 \pm 6$ Å. Independent measurements by interference microscopy on the LB film of optical density $A_m = 1.65$ gave the film thickness as 0.14 μm. Since our experience has shown that the maximum optical density of films is always proportional to the number of transferred bilayers, the ratio of the optical density to the thickness (a calibration coefficient for MEL63) was found to be: $\delta = A_m/d \approx 1.2 \times 10^{-3}$ Å^{-1}. This coefficient allows us to estimate a film thickness from routine measurements of the film absorbance.

Figure 4 shows the first order diffraction efficiency of the probe beam with *s* and *p* polarization as a function of the time of grating recording by two convergent Ar laser beams, both having the same polarizations, either *s* (left) or *p* (right). The power of the initial Ar beam was fixed in the two cases at $P_0 = 6$ mW and all experimental points were taken from only two laser spots on the sample, one for each of the two polarizations. At the probe beam wavelength, the grating is a pure phase grating because red light is not absorbed by our films—see figure 1. This has also been checked with mutually perpendicular polarizations of the two convergent writing beams. In this case, only the phase grating may be recorded since the light intensity in the interference pattern on the sample is the same and only light polarization is spatially modulated [28].

A view of diffraction gratings under a polarizing microscope is shown in figure 5. The grating shown in figure 5 (*a*) was recorded by two *s* beams with total power 30 mW. Using a compensator, the local directions

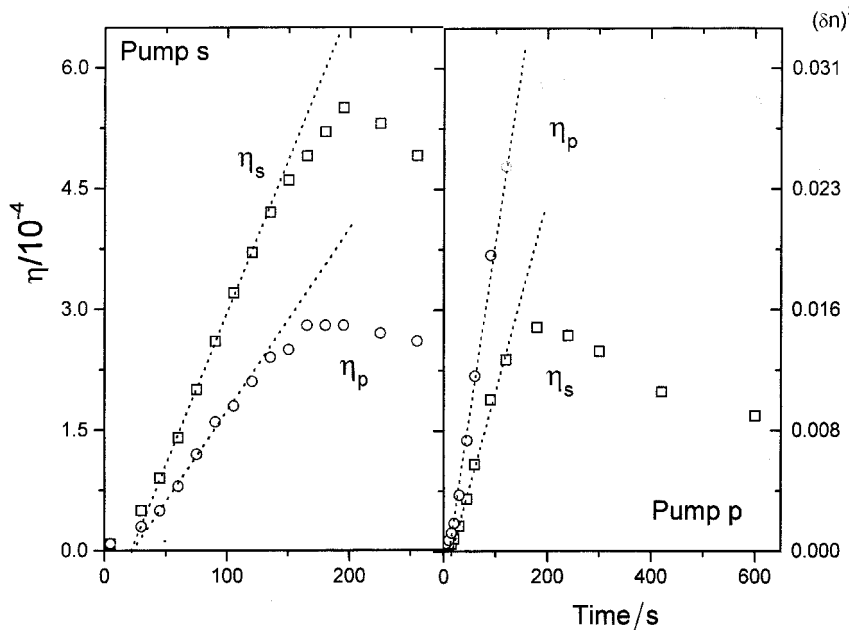

Figure 4. First order diffraction efficiency of the *s* and *p* polarized probe beam as a function of time of grating recording with the same, either *s* (left) or *p* (right) polarizations of the two convergent pump beams (initial Ar beam power $P_0 = 6$ mW, at $\lambda = 514$ nm). On the right scale δn is the difference in refraction indices between illuminated and dark areas.

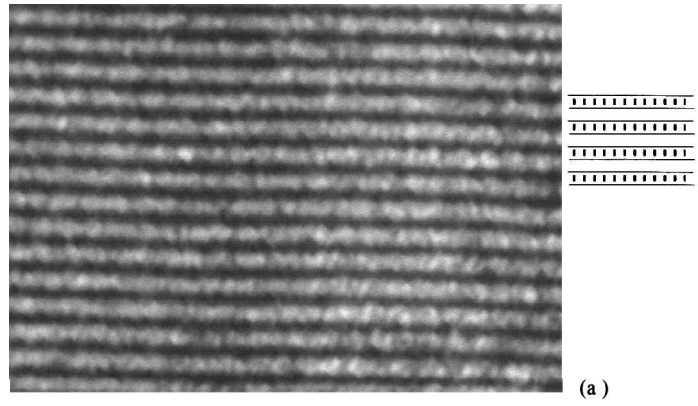

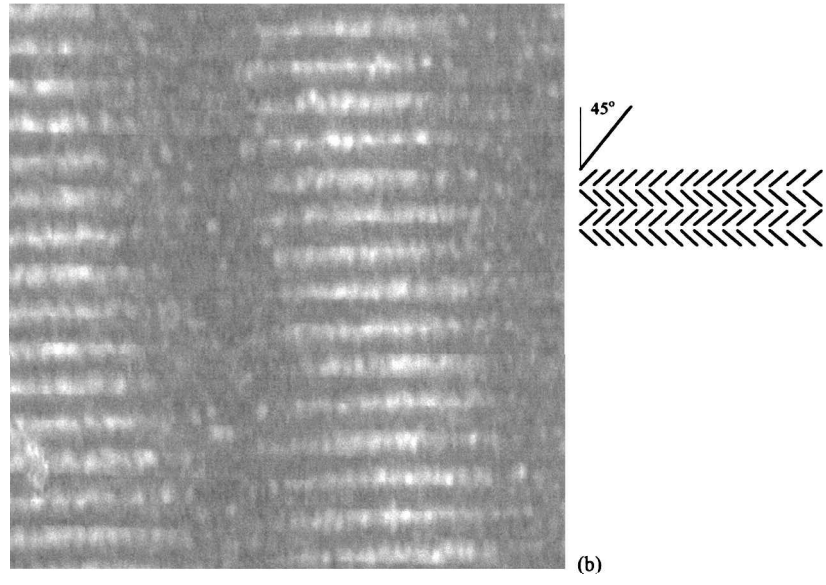

Figure 5. A diffraction grating on a LB film viewed using a polarizing microscope (crossed polarizers) and the schemes of molecular orientation: (*a*) *ss* polarizations of the recording beams, black and bright stripes correspond to oriented and non-oriented domains; (*b*) *sp* polarizations of the recording beams (Ar beam power $P_0 = 30$ mW, time 60 s).

of the optical axes and birefringence of the LB film may be found. In the white stripes corresponding to maximum light intensity, the direction of the optical axis (projection of the molecular long axes on the substrate plane) is almost perpendicular to the electric vector of the recording beams. This direction is shown in the scheme, figure 5(*a*). The optical anisotropy in the *s* or *p* spots (without grating) $n_a \approx 0.33$–0.37. This value corresponds to the saturation of the diffraction efficiency of the grating shown in figure 4 and is less than the maximum birefringence possible in this system (about 0.4 [24]) since the chromophores are tilted with respect to the substrate plane.

Quite a different picture is observed for the *sp* grating, figure 5(*b*). It is known that, in this case, the light polarization is changing on translation along the **q** direction in the following sequence: linear polarization with the electric vector **e** at an angle of 45° to the plane of incidence, elliptical polarization, circular polarization, elliptical again, linear polarization with the electric vector **e** at an angle of − 45° to the plane of incidence, elliptical again, and so on. The light-induced reorientation of the chromophores to some extent follows this sequence since the azo-chromophores always 'prefer' to be perpendicular to **e**. In fact, our birefringence measurements have indicated that they acquire only two favourable orientations at ±45° to the incidence plane, as shown in the sketch in figure 5(*b*).

3.2. *Liquid crystal gratings*

After cooling from the isotropic into the nematic phase, high contrast gratings were observed under a microscope. The liquid crystal is certainly oriented by the anisotropic surface of the LB film. In figure 6 two such images are displayed, for *ss* (*a*) and *pp* (*b*) polarizations of the recording beams. The liquid crystal texture on the *pp* spot is almost the same as that on the *ss* spot, but the direction of orientation is different. In the *ss* spots, on illuminated areas (dark stripes), the director is oriented perpendicular to stripes, along the wavevector **q** of the grating; that is, oppositely to the case of orientation by a mechanical relief. For the *pp* spot the director is oriented along the illuminated stripes. Sketches of the director orientation are shown in figure 6(*b*). Due to the sine wave distribution of rather a high light intensity, non-illuminated stripes are narrower and only one disclination line is observed separating illuminated areas (one line per period of the grating). The line is clearly seen in the *ss* spot and follows an irregular 'chain of islands' formed by non-oriented liquid crystal.

More precise study of the director orientation shows that for the *ss* spot there is some deviation of the director from the direction of the grating wave vector. We do not think that this is related to the influence of the grating wave vector for the following two reasons: first, our AFM measurements did not reveal any relief; secondly, the grating wave vector is so small (only 10^3 cm^{-1}) that

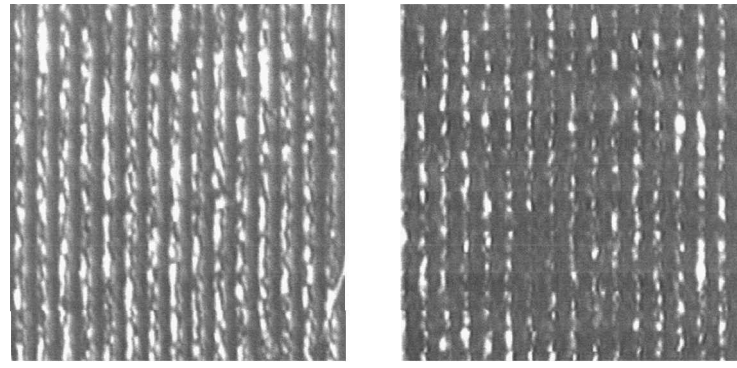

(a)

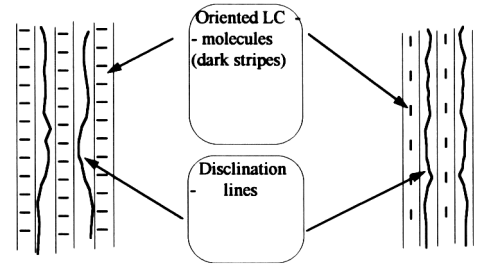

(b)

Figure 6. (*a*) Images of liquid crystal gratings between crossed polarizers for *ss* (left) and *pp* (right) polarizations of the recording beams (Ar beam power $P_0 = 30$ mW, time 60 s). The wavevector of the gratings is parallel to the polarizer, and the grating period is 10 μm. (*b*) The scheme of director orientation and location of disclinations in the gratings.

had the amplitude of the relief A been even comparable with the film thickness ($2A = 400$ Å), the product A^2q^3 would be very small and might provide an anchoring energy of only about 10^{-6} erg cm^{-2} [6]. Therefore, another reason for the director deviation has to be found, and we believe that it might be related to material flow during filling the cell (even using the isotropic phase).

The liquid crystal orientation on the *sp* grating is quite different from those described above. Two images of such a grating are shown in figure 7 for different angles of the grating wave vector with respect to the crossed polarizers. The two sets of equally wide stripes may be darkened separately when the polarizers are crossed. The stripes are separated by disclination lines about 0.5 μm wide, figure 7 (*a*) (top), and so, in this case, we observe two lines per grating period. The latter are better seen when the polarizers are installed at 45° to each other, figure 7 (*a*) (bottom): now the images of the disclinations are broadened, bright lines appear in their centres and the period of the optical pattern decreased by a factor of 2. The corresponding scheme in figure 7 (*b*) shows that the director follows the direction of the azo-chromophores in the irradiated LB film and acquires two favourable orientations, at +45° and −45° to the incidence plane.

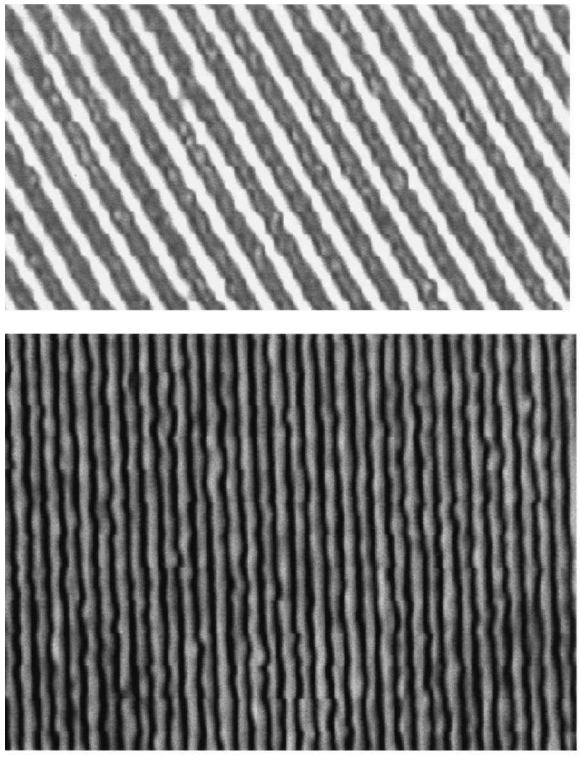

(a)

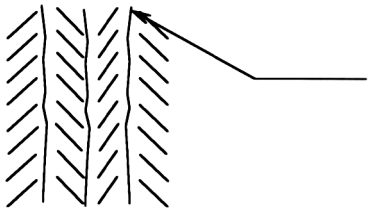

(b)

Figure 7. (*a*) Images of the liquid crystal grating (period = 10 μm) for *sp* polarizations of the recording beams (Ar beam power $P_0 = 30$ mW, time 60 s). Top: crossed polarizers (period of the stripes coincides with the grating period). Bottom: polarizer and analyser at 45° to each other (period of stripes is a factor of 2 less than the grating period). The grating wavevector is always parallel to the analyzer. (*b*) Scheme of director orientation and location of disclinations to the grating.

Therefore, such a grating represents a new type of quasi-bistable surface for liquid crystal orientation different from genuinely bistable cases such as, for example, cleavages of NaCl and mica [29] or bistable SiO surfaces [10]. Locally our *sp*-grating is a combination of the two sets of stripes orienting the liquid crystal differently, but taking a 'bird's eye view', say from distances much larger than a grating period, the orientational state of the liquid crystal might be bistable due to competition of neighbouring stripes to provide a unique easy direction (the elastic energy will be gained by eliminating the disclination lines).

3.3. *Pretilt angle and anchoring energy measurements*

The pretilt angle ϑ_s (taken from the substrate plane) at the planar interface ($z = 0$) may be determined from the phase retardation $\Phi = d\langle\Delta n\rangle$ of a hybrid cell of known thickness d under the assumption of infinitely strong anchoring at the homeotropic interface ($z = d$):

$$\langle d\Delta n\rangle(\vartheta_s) = \int_0^d \left[1 - \frac{n_\parallel^2 - n_\perp^2}{n_\parallel^2}\cos^2\vartheta(z)\right]^{-1/2} n_\perp \mathrm{d}z - n_\perp d \qquad (1)$$

Assuming the linear dependence of the director angle $\vartheta(z)$ upon cell thickness $0 < z < d$ that is only true in the one-constant approximation for elastic moduli, $K = K_{11} = K_{33}$, we calculate the average retardation of the cell $\langle d\Delta n\rangle(\vartheta_s)$ from equation (1) and find ϑ_s from comparison with the experimental values of the retardation of the cell in zero field. The latter may be found either using a microscope with a compensator or on an optical bench with a He-Ne laser (see below).

For the anchoring energy measurements, we measured the field-dependent retardation using a technique involving $\lambda/4$-plate rotation [25]. A polarized He-Ne laser beam was passed through a cell (or a diffraction spot in the cell) and then modulated by a rotating (frequency 80 Hz) $\lambda/4$-plate and passed through an analyser. The modulated

beam was detected by a photodiode at the first and second harmonic by a virtual lock-in amplifier made by appropriate programming of a multimedia card of an IBM computer (PhysLab software by S. Palto). The sine-form voltage at frequency 2 kHz with a linearly increasing (or decreasing) amplitude was delivered to the cell from the same computer and amplified if necessary. An oscillating dependence of the detected signal amplitude on the applied voltage was recalculated in order to give the phase retardation as a function of voltage.

Figure 8 shows the measured values of the phase retardation (on a logarithmic scale) as functions of the applied electric field for four Ar laser illuminated spots recorded in different regimes, without grating (*s* spot) and with gratings of different polarizations (*ss*, *pp*, *sp* spots). The zero-field retardation values and the corresponding pretilt angles are shown in the table.

The same curves processed with our software allow for determination of the 5CB anchoring energy at different gratings. To do this the experimental curves were fitted to the numerically solved standard equations describing a semi-infinite liquid crystal layer planarly

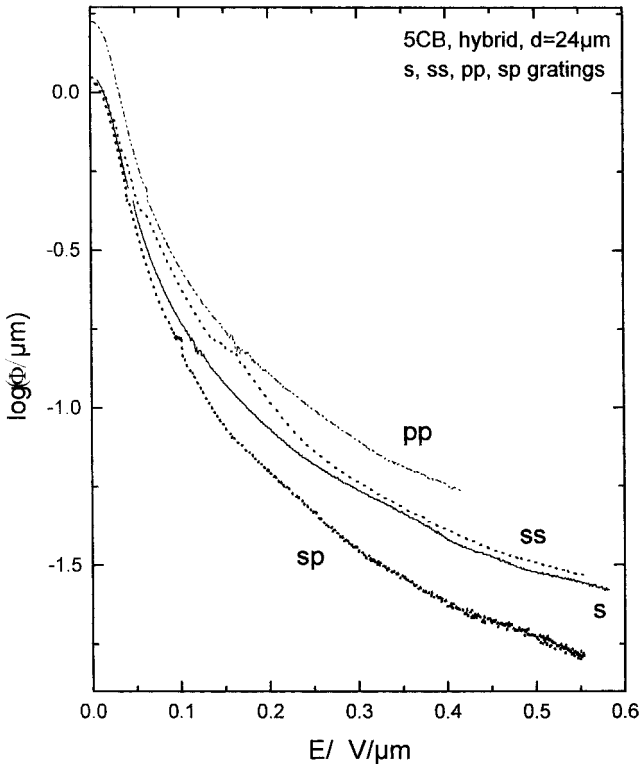

Figure 8. Experimental curves for the phase retardation (on a logarithmic scale) as functions of the applied electric field for four Ar laser illuminated spots recorded in different regimes, without grating (*s* spot) and with gratings of different polarizations (*ss*, *pp*, *sp* spots). Hybrid 24 μm thick cell filled with 5CB.

Table 1. Zero-field phase retardation $\Delta n d_{\max}$, the pretilt angle ϑ_s and the anchoring energy for different gratings (spots) in a hybrid 24 μm thick cell.

Grating	$\Delta n d$/μm	ϑ_s/°	W_0/erg cm^{-2} (fitted ϑ_f/°)
s spot	1.125	28.8	0.15 (26)
ss spot	1.572	13.1	0.08 (13)
pp spot	1.682	9	0.15 (7)
sp spot	0.996	33.1	0.04 (30)

anchored at $z = 0$ [26]. As in [26], a large dielectric anisotropy, large surface deviation angles and different elastic moduli were explicitly taken into consideration. In addition, the Rapini form of the surface energy at the planar interface was taken in a more general form

$$W(\vartheta) = (W_0/2)\sin^2(\vartheta - \vartheta_s) \qquad (2)$$

which takes into account a pretilt angle ϑ_s. The calculations of the field dependence of the phase retardation were made for the following parameters of 5CB [1, table 1]: $K_{11} = 6.4 \times 10^{-7}$ dyn, $K_{33} = 1.0 \times 10^{-7}$ dyn, $n_\parallel = 1.7063$, $n_\perp = 1.5309$, $\varepsilon_\parallel = 19.7$, $\varepsilon_\perp = 6.7$ with two free parameters W_0 and ϑ_s varied. Since our cell is of a finite thickness, the comparison of the calculated and experimental curves makes sense only for rather high fields when the distortion region (ϑ angle different from $\pi/2$), expressed by the electric coherence length ($\varepsilon_a = \varepsilon_\parallel - \varepsilon_\perp = 13$)

$$\xi = \frac{1}{E}\left(\frac{4\pi K_{11}}{\varepsilon_a}\right)^{1/2}, \qquad (3)$$

is considerably less than the cell thickness.

Figure 9 shows the experimental phase retardation (scatter graphs) as a function of the electric coherence length in the range of $\xi \ll d = 24$ μm, together with the best fitting curves (dotted lines displayed in the vicinity of each experimental curve). The fitting seems quite satisfactory if we take into account the difficulties of the phase retardation measurements on small spots where gratings have been recorded. The parameters of fitting are also given in the table. Although there is a certain correlation between the tilt angle ϑ_f taken for the fitting and the real tilt angle ϑ_s, the former is generally higher than the latter. This is not surprising in view of the semi-infinite medium model which should not be good for small fields corresponding to the maximum retardation values. On the contrary, the values of the anchoring

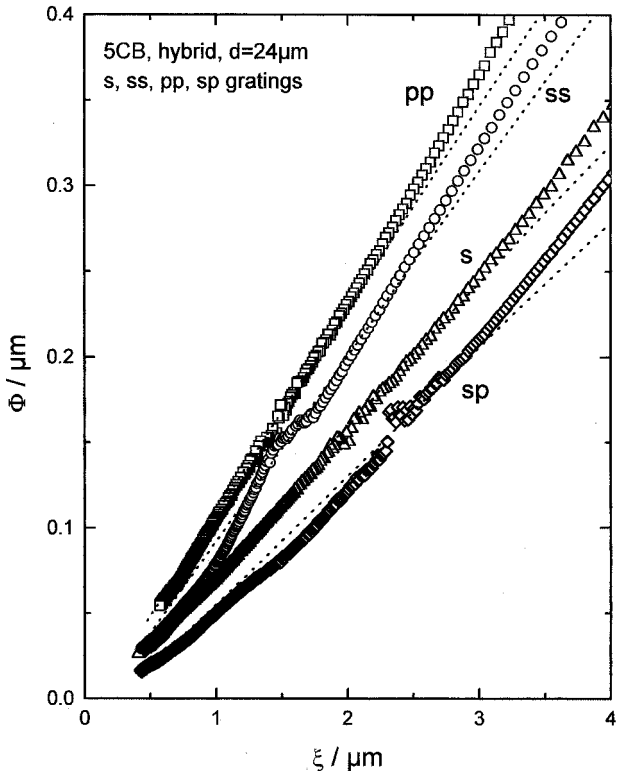

Figure 9. The same phase retardation data as in figure 8 presented as functions of the electric coherence length (scatter graphs), together with the best fitting curves (dotted lines displayed in the vicinity of each experimental curve). The fitting parameters are given in the table.

energy are mostly determined by the $\Phi(\xi)$ slope at higher fields and seem to be correct. Thus we may conclude that LB gratings provide rather weak anchoring in the range 0.04–0.15 erg cm^{-2} which may be controlled by the recording regime. Therefore, the gratings are very promising for a study of orientational multistability effects and storage devices described earlier [26, 30].

4. Conclusion

In conclusion, (i) we have recorded holographic gratings on photosensitive Langmuir–Blodgett films with different polarizations of the writing Ar laser beams and characterized the gratings by various techniques (UV spectroscopy, birefringence, AFM); (ii) it has been shown that the gratings orient a nematic liquid crystal with the director parallel to the axes of chromophores, predetermined by film irradiation in all the cases studied (*ss*, *pp* or *sp* gratings); (iii) *sp* gratings provide two equivalent easy directions for liquid crystal orientation at 90° with respect to each other, and hence a new type of a quasi-bistable anchoring interface has been prepared; (iv) the pretilt angle (from 9° to 33°) and the anchoring energy (from 0.04 to 0.15 erg cm^{-2}) were shown to be controlled by the grating recording regime. Liquid crystal orienting layers with such a small photoelectrically controlled anchoring energy are very promising for nematic displays using multistable and storage orientational effects.

We are grateful to Prof. R. Bartolino and Dr M. Giocondo for useful discussions, to Dr N. Scaramuzza for a help with spectral measurements and to Dr S. G. Yudin for his help in the film deposition. The work has been carried out in the framework of the Copernicus (grant no. IC15-CT96-0744) program and INFM 'Progetto Sud'.

References

[1] Blinov, L. M., and Chigrinov, V. G., 1993, *Electrooptic Effects in Liquid Crystal Materials* (New York: Springer).
[2] Dydyusha, A. G., Kozenkov, V. M., Marusii, T. Ya., Reznikov, Yu. A., Reshetnyak, V. Yu., and Khizhnyak, A. I., 1991, *Ukr. Fiz. Zh.*, **36,** 1059.
[3] Schadt, M., Schmit, K., Kozenkov, V., and Chigrinov, V., 1992, *Jpn. J. appl. Phys.*, **31,** 2155.
[4] Gibbons, W., Shannon, P., Sun, S.-T., and Swetlin, B., 1991, *Nature*, **351,** 49.
[5] Flanders, D. C., Shaver, D. C., and Smith, H. I., 1978, *Appl. Phys. Lett.*, **32,** 597.
[6] Berreman, D., 1972, *Phys. Rev. Lett.*, **28,** 1683.
[7] Nakamura, M., and Ura, M., 1981, *J. appl. Phys.*, **52,** 210.
[8] Pidduk, A. J., Haslam, S. D., Bryan-Brown, G. P., Bannister, R., and Kitely, I. D., 1997, *Appl. Phys. Lett.*, **71,** 2907.
[9] Bryan-Brown, G. P., Towler, M. J., Bancroft, M. S., and McDonnell, D. G., 1994, *Proc. IDRC, Sid'94*, p. 209.
[10] Barberi, R., and Durand, G., 1997, *Handbook of Liquid Crystal Research*, edited by P. Collings and J. Patel (Oxford: Oxford University Press) p. 567.
[11] Dydyusha, A. G., Reznikov, Yu. A., and Reshetnyak, V. Yu., 1995, *Mol. Mater.*, **5,** 183.
[12] Dydyusha, A. G., Khizhnyak, A. I., Marusii, T. Ya., Reznikov, Yu. A., Yaroshchuk, O., Reshetnyak, V. Yu., Park, W., Kwon, S., Shin, H., and Kang, D., 1995, *Mol. Cryst. liq. Cryst.*, **263,** 399.
[13] Proust, J. E., Ter-Minassian-Saraga, L., 1977, *Solid State Commun.*, **11,** 1227.
[14] Luk'yanchenko, E. S., Khozhanov, V. V., and Kozunov, V. A., 1985, *Kristallografiya*, **31,** 751.
[15] Blinov, L. M., and Sonin, A. A., 1987, *Langmuir*, **3,** 660.
[16] Ikeno, H., Oh-Saki, A., Nitto, M., Ozaki, N., Nakaya, K., and Kobayashi, S., 1998, *Jpn. J. appl. Phys.*, **54,** L475.
[17] Nishikata, T., Morikawa, A., Takiguchi, T., Kanemoto, A., Kakimoto, M., and Imai, T., 1988, *Jpn. J. appl. Phys.*, **54,** L1163.
[18] Chen, J., Vithana, H., Johnson, D., Albarici, A., Lando, J., Mann, J. A., and Kakimoto, M., 1996, *Mol. Cryst. liq. Cryst.*, **275,** 49.
[19] Ishimura, K., Susuki, Y., Seki, T., Kawanishi, Y., and Aoki, N., 1988, *Langmuir*, **4,** 1214.

[20] Seki, T., Sakurai, M., Kawanishi, Y., Susuki, Y., Tamaki, T., Ishimura, K., Fukuda, R., and Hiramatsu, H., 1992, *Thin Solid Films*, **210/211,** 836.
[21] Barnik, M. I., Kozenkov, V. M., Shtykov, N. M., Palto, S. P., and Yudin, S. G., 1989, *J. Mol. Electr*., **5,** 53.
[22] Palto, S. P., Yudin, S. G., Germain, C., and Durand, G., 1995, *J. Phys. II Fr*., **5,** 133.
[23] Blinov, L. M., Cipparrone, G., Palto, S. P., Shtykov, N. M., and Yudin, S. G., 1998, *Mol. Mater*., **9** (in the press).
[24] Blinov, L. M., Cipparrone, G., and Palto, S. P., 1998, *Int. J. nonlin. opt. Phys*., **7** (in the press).
[25] Palto, S. P., Barberi, R., Iovane, M., Lazarev, V. V., and Blinov, L. M., 1998, *Mol. Mater*. (to be published).
[26] Yang, K. H., 1983, *J. Phys. Fr*., **44,** 1051.
[27] Schöndorf, M., Mertesdorf, M., and Lösche, M., 1996, *J. phys. Chem*., **100,** 7558.
[28] Eichler, H. J., Günter, P., and Pohl, D. W., 1986, *Laser-Induced Dynamic Gratings* (New York, Tokyo: Springer Verlag).
[29] Blinov, L. M., and Sonin, A. A., 1990, *Mol. Cryst. liq. Cryst*., **179,** 13.
[30] Ong, H. L., Meyer, R. B., and Hurd, A. J., 1984, *J. appl. Phys*., **57,** 2809.